CHEMISTRY
A EUROPEAN JOURNAL

FULL PAPER

DOI: 10.1002/chem.201200456

Control of Interpenetration and Gas-Sorption Properties of Metal–Organic Frameworks by a Simple Change in Ligand Design

Thazhe Kootteri Prasad and Myunghyun Paik Suh*[a]

Abstract: In metal–organic framework (MOF) chemistry, interpenetration greatly affects the gas-sorption properties. However, there is a lack of a systematic study on how to control the interpenetration and whether the interpenetration enhances gas uptake capacities or not. Herein, we report an example of interpenetration that is simply controlled by the presence of a carbon–carbon double or single bond in identical organic building blocks, and provide a comparison of gas-sorption properties for these similar frameworks, which differ only in their degree of interpenetration. Noninterpenetrated (**SNU-70**) and doubly interpenetrated (**SNU-71**) cubic nets were prepared by a solvothermal reaction of $[Zn(NO_3)_2]\cdot 6H_2O$ in *N*,*N*-diethylformamide (DEF) with 4-(2-carboxyvinyl)-benzoic acid and 4-(2-carboxyethyl)-benzoic acid, respectively. They have almost-identical structures, but the noninterpenetrated framework has a much bigger pore size (ca. 9.0×9.0 Å) than the interpenetrated framework (ca. 2.5×2.5 Å). Activation of the MOFs by using supercritical CO_2 gave **SNU-70′** and **SNU-71′**. The simulation of the PXRD pattern of **SNU-71′** indicates the rearrangement of the interpenetrated networks on guest removal, which increases pore size. **SNU-70′** has a Brunauer–Emmett–Teller (BET) surface area of 5290 $m^2 g^{-1}$, which is the highest value reported to date for a MOF with a cubic-net structure, whereas **SNU-71′** has a BET surface area of 1770 $m^2 g^{-1}$. In general, noninterpenetrated **SNU-70′** exhibits much higher gas-adsorption capacities than interpenetrated **SNU-71′** at high pressures, regardless of the temperature. However, at $P<1$ atm, the gas-adsorption capacities for N_2 at 77 K and CO_2 at 195 K are higher for noninterpenetrated **SNU-70′** than for interpenetrated **SNU-71′**, but the capacities for H_2 and CH_4 are the opposite; **SNU-71′** has higher uptake capacities than **SNU-70′** due to the higher isosteric heat of gas adsorption that results from the smaller pores. In particular, **SNU-70′** has exceptionally high H_2 and CO_2 uptake capacities. By using a post-synthetic method, the C=C double bond in **SNU-70** was quantitatively brominated at room temperature, and the MOF still showed very high porosity (BET surface area of 2285 $m^2 g^{-1}$).

Keywords: carbon dioxide · adsorption · hydrogen · interpenetration · metal–organic frameworks

Introduction

Porous metal–organic frameworks (MOFs) have received considerable attention due to their high surface areas and excellent gas-sorption properties.[1–3] In MOF chemistry, control of the interpenetration is of high importance because the degree of interpenetration significantly affects the gas-sorption properties of the material.[2] There have been a few reports of methods to control the interpenetration of MOFs. Some reported methods include the addition of a template during the synthesis,[4,5] rational design of ligands,[6,7] and adjustment of the reaction conditions, such as the concentration of building blocks and temperature.[8] In particular, if the length of the ligand is elongated then the MOF has a better tendency to form an interpenetrated structure. However, when using ligands with similar length it is difficult to predict which framework will be interpenetrated and which will be noninterpenetrated. Previously, it was reported that interpenetrated structures showed higher gas-sorption capacities for N_2 and H_2 gases at 77 K under both low and high pressures, and at 298 K under high pressure.[4,7a] In contrast, theoretical calculations have predicted that noninterpenetrated structures should have better gas-sorption capacities than interpenetrated structures.[9] Despite these contradictory arguments, it is difficult to prove which is the more general case because gas-sorption properties should be compared between frameworks with similar structures that only differ in their degree of interpenetration. However, such cases are difficult to find.[4,7]

Herein, we report an example of interpenetration and consequent gas-sorption properties of MOFs, which is simply controlled by the presence of a carbon–carbon double or single bond in identical organic building blocks (Scheme 1). This is significant in several respects: 1) reports of the systematic comparison of gas sorption properties for similar frameworks that differ only in the degree of interpenetration are very rare; 2) highly porous **SNU-70′** is presented, which has an extraordinary high surface area and ex-

[a] Dr. T. K. Prasad, Prof. M. P. Suh
Department of Chemistry, Seoul National University
Seoul 151-747 (Republic of Korea)
Fax: (+82) 28868516
E-mail: mpsuh@snu.ac.kr

Supporting information for this article is available on the WWW under http://dx.doi.org/10.1002/chem.201200456.

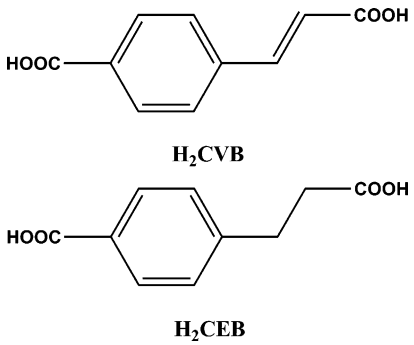

H_2CVB

H_2CEB

Scheme 1. Ligands used in **SNU-70** and **SNU-71**.

ceptionally high H_2, CO_2, and CH_4 gas-sorption capacities; 3) the rearrangement of the interpenetrated networks upon guest removal, which leads to expansion of pore size, is revealed; 4) the post-synthetic bromination of the C=C double bonds in the MOF is reported, in particular quantitatively and at room temperature.

Results and Discussion

Syntheses and X-ray crystal structures of SNU-70 and SNU-71: Pale-yellow cubic crystals of $[Zn_4O(CVB)_3]\cdot 13\,DEF\cdot 2\,H_2O$ (**SNU-70**) and $[Zn_4O(CEB)_3]\cdot 6\,DEF\cdot H_2O$ (**SNU-71**) were obtained by heating $[Zn(NO_3)_2]\cdot 6\,H_2O$ with 4-(2-carboxyvinyl)benzoic acid (H_2CVB) or 4-(2-carboxyethyl)benzoic acid (H_2CEB), respectively, at 105 °C for 12 h in *N*,*N*-diethylformamide (DEF). X-ray crystal structures (Figure 1) of **SNU-70** and

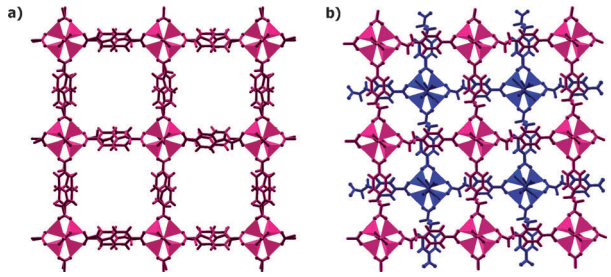

Figure 1. X-ray crystal structures of: a) noninterpenetrated **SNU-70**, and b) doubly interpenetrated **SNU-71**. The interpenetrated two independent frameworks are represented in red and blue.

SNU-71 indicate that they have similar cubic-net structures that are constructed from $[Zn_4O]^{6+}$ octahedral secondary building units (SBUs) and linear dicarboxylate linkers, similarly to MOF-5.[7b] In both frameworks, the distances between the nearest $[Zn_4O]$ clusters in a cubic net is 15 Å. However, **SNU-70** has a noninterpenetrated structure whereas **SNU-71** has a doubly interpenetrated structure. Noninterpenetrated **SNU-70** generates square channels with dimensions of approximately 9.0×9.0 Å in three orthogonal directions, which is much larger than those of interpenetrated **SNU-71** (ca. 2.5×2.5 Å). The guest solvent molecules in **SNU-70** and **SNU-71** could not be located from the difference map due to significant thermal disorder, and were determined by elemental analyses and thermogravimetric analysis (TGA) data. As expected, the amount of guest solvent molecules per formula unit in doubly interpenetrated **SNU-71** is nearly half that in **SNU-70**.

Activation of the MOFs by using supercritical CO_2 gives completely desolvated materials, $[Zn_4O(CVB)_3]$ (**SNU-70′**) and $[Zn_4O(CEB)_3]$ (**SNU-71′**). The powder X-ray diffraction (PXRD) patterns indicate that **SNU-70** retains its structure but **SNU-71** undergoes a structural rearrangement upon removal of the guest solvent molecules (Figure 2).[10] The pos-

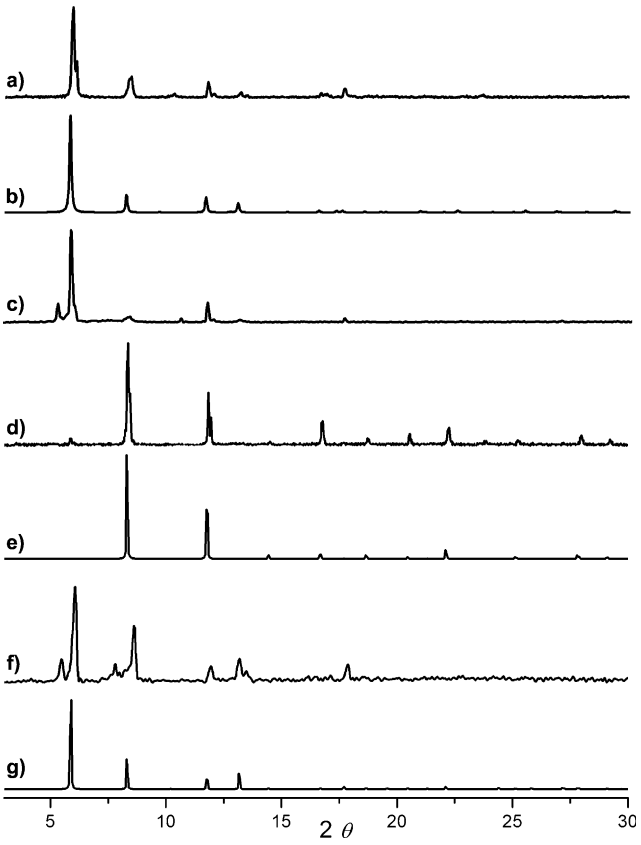

Figure 2. PXRD patterns: a) as-synthesized **SNU-70**, b) pattern of **SNU-70** simulated based on X-ray crystallographic data, c) **SNU-70′** resulting from supercritical CO_2 treatment of **SNU-70**, d) as-synthesized **SNU-71**, e) pattern of **SNU-71** simulated based on X-ray crystallographic data, f) **SNU-71′** resulting from supercritical CO_2 treatment of **SNU-71**, and g) simulated pattern of the modeled structure of **SNU-71′**, which is described in Figure 3.

sible structure of **SNU-71′** was simulated from the PXRD pattern by using the Materials Studio program.[11] Upon guest removal, the two interpenetrated frameworks move closer due to the hydrogen-bonding interactions of C–H···O, which enlarges the pore size from 2.5×2.5 Å to 6.0×5.8 Å, as shown in Figures 3 and 4.

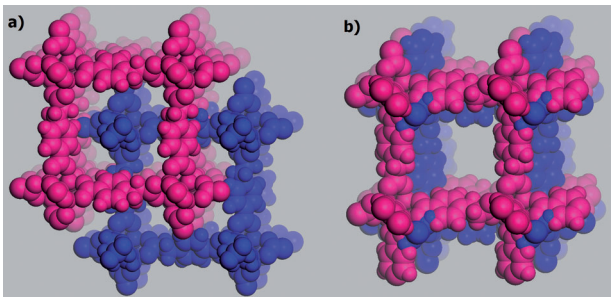

Figure 3. Simulated structural transformation of **SNU-71** on removal of guest molecules. a) X-ray crystal structure of **SNU-71**, and b) simulated structure of desolvated **SNU-71′** based on its PXRD pattern.

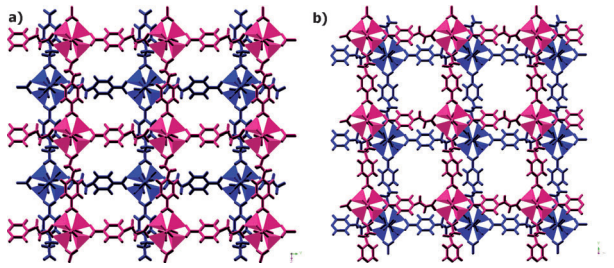

Figure 4. Simulated structure of **SNU-71′**. a) View along the *ac* or *bc* plane, and b) view along the *ab* plane.

Gas-sorption properties: Gas-sorption isotherms of **SNU-70′** and **SNU-71′** were measured for N_2, H_2, CO_2, and CH_4, and the data are summarized in Table 1 together with the data for other MOFs for comparison. Noninterpenetrated **SNU-70′** has a pore volume of 2.17 $cm^3 g^{-1}$ and a BET surface area of 5290 $m^2 g^{-1}$ (Langmuir 6100 $m^2 g^{-1}$), which is the highest of all MOFs with cubic-net structures and is comparable to the highest values reported so far for MOFs such as MOF-210[1] (BET 6240 $m^2 g^{-1}$) and NU-100 (BET 6143 $m^2 g^{-1}$).[12] Although the pore size of as-synthesized **SNU-71** is much smaller than the kinetic diameter of N_2 (3.64 Å), the desolvated **SNU-71′** sample adsorbs a large amount of N_2 due to the increase in pore size on desolvation, as discussed earlier. The **SNU-71′** sample has a pore volume of 0.709 $cm^3 g^{-1}$ and a BET surface area of 1770 $m^2 g^{-1}$ (Langmuir 1923 $m^2 g^{-1}$).

The H_2 adsorption isotherms of **SNU-70′** and **SNU-71′** were measured at 77 and 87 K (Figure 5b), and the isosteric heats (Q_{st}) of the H_2 adsorption were estimated from the data by using the virial equation.[13] In contrast to the N_2 adsorption, **SNU-71′** adsorbs a higher amount of H_2 gas than **SNU-70′** at 77 and 87 K below $P<1$ atm. This might be related to the isosteric heat of H_2 adsorption in **SNU-71′**, which is approximately 2 kJ mol^{-1} higher than that of **SNU-70′**. The smaller pore size of **SNU-71′** increases the overlap potential between the framework and hydrogen.[14] However, at 77 K and high pressure, the H_2 uptake capacity of **SNU-70′** becomes greater than that of **SNU-71′** (Figure 6). The excess H_2 uptake capacity of **SNU-70′** is greater than **SNU-71′** by a factor of 1.85 at 77 K and 1.54 at 298 K. The total H_2 uptake capacity of **SNU-70′** is 2.1 times greater than that of **SNU-71′** at 77 K and 2.4 times greater at 298 K. In particular, the H_2 uptake capacity of **SNU-70′** at 77 K and high pressure is extraordinarily high, with an excess of 73.8 mg g^{-1} (total 117.4 mg g^{-1}) at 77 K and 70 bar. This is comparable to the highest reported H_2 uptake capacities, such as 99.5 mg g^{-1} excess at 56 bar (total 164 mg g^{-1} at 70 bar) for NU-100,[12] 86 mg g^{-1} excess (total 176 mg g^{-1} at 80 bar) for MOF-210,[1] 74.0 mg g^{-1} excess (total 163 mg g^{-1} at 80 bar) for MOF-200,[1] and 81.0 mg g^{-1} excess (total 110.6 mg g^{-1} at 90 bar) for **SNU-77H**.[15]

The CO_2 gas sorption isotherms of **SNU-70′** and **SNU-71′** were measured at various temperatures (Figure 7). At 195 K and 1 atm, **SNU-70′** shows a S-shaped isotherm similar to MOF-5, due to the attractive electrostatic interactions between the CO_2 molecules.[16] **SNU-70′** exhibits a CO_2 adsorption capacity of 2214 mg g^{-1} at 195 K and 1 atm, which is about four times greater than that of **SNU-71′**, in accordance with the fact that N_2 adsorption is higher for **SNU-70′** than **SNU-71′** at 77 K and $P<1$ atm. The CO_2 uptake capacity of **SNU-70′** is higher than the reported value for MOF-5 (1500 mg g^{-1}) and pmg-MOF-5 (2000 mg g^{-1}) under

Table 1. Gas adsorption properties of **SNU-70′** and **SNU-71′**, with comparisons to other MOFs.

	SNU-70′	**SNU-71′**	**SNU-77H**[15]	**MOF-5**[1,2a]	**MOF-177**[1]	**MOF-210**[1]	**NU-100**[12]	**PCN-68**[24]
BET S.A. [$m^2 g^{-1}$]	5290	1770	3670	4400	4500	6240	6143	5109
V_{pore} [$cm^3 g^{-1}$]	2.17	0.709	1.52	1.55	1.89	3.60	2.82	2.13
H_2, 77 K [mg g^{-1}][a]	12.4	14.4	17.9	1.32	1.25[27]	–	18.2	18.7
H_2, 77 K [mg g^{-1}][b]	73.8/117.4/70	39.9/54.6/70	81.0/110/90	53/82/80	73/116/80	86/176/80	99.5/164/70	73.2/135/50
H_2, 298 K [mg g^{-1}][b]	4.0/14.5/70	2.6/6.1/70	5.0/11.9/90	–	–	–	–	10.1/29/90
Q_{st} (H_2) [kJ mol^{-1}][c]	5.12	7.22	7.05	4.8	–	–	6.1	6.09
CO_2, 195 K [mg g^{-1}][a]	2210	580	1690	1500[17]	–	–	–	–
CO_2, 298 K [mg g^{-1}][a]	35	46	39	46[21]	35[21]	–	–	–
CO_2, 298 K [mg g^{-1}][b]	1420/1640/45	493/564/45	933/1030/40	864/1030/50	1356/1550/80	2396/2870/50	2043/2315/40	1338/1804/100
Q_{st} (CO_2) [kJ mol^{-1}][c]	17.2	17.8	19.9	16.5[25]	14[28]	–	–	21.2
CH_4, 195 K [mg g^{-1}][a]	39	49	87	–	–	–	–	–
CH_4, 298 K [mg g^{-1}][a]	4.9	5.2	6.2	–	–	–	–	–
CH_4, 298 K [mg g^{-1}][b]	168/224/45	101/121/45	142/173/35	165/250/80	243/345/80	264/475/80	–	186/465/100
Q_{st} (CH_4) [kJ mol^{-1}][c]	9.4	14.6	14.3	12.2[26]	–	–	–	15.2

[a] At 1 atm. [b] At high pressure. Excess/total capacity/pressure in bar. [c] Isosteric heat of adsorption at zero coverage.

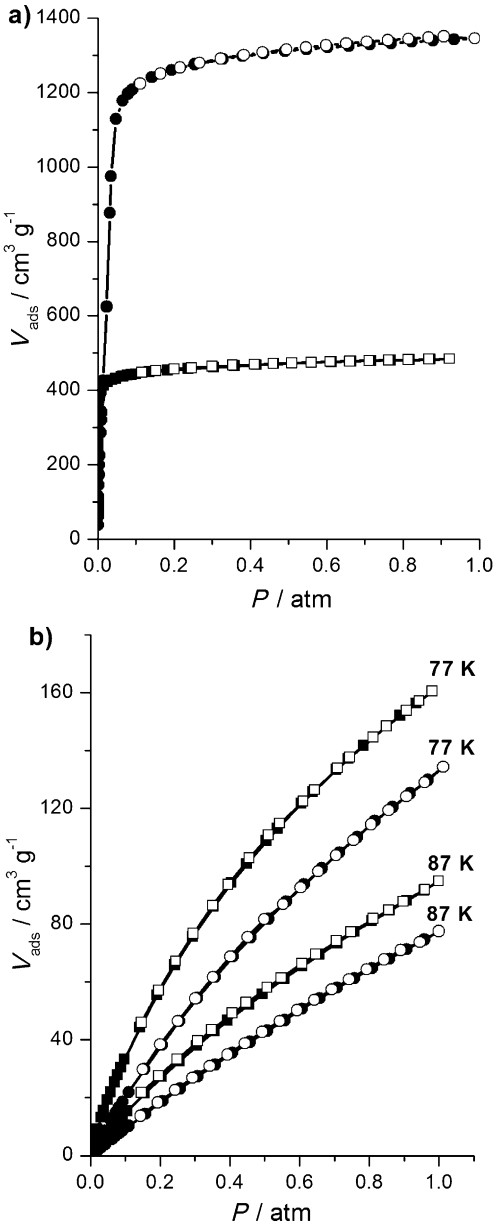

Figure 5. The N_2 and H_2 adsorption isotherms of **SNU-70′** (●, ○) and **SNU-71′** (■, □). a) N_2 at 77 K, and b) H_2 at 77 and 87 K. Filled shapes: adsorption; open shapes: desorption.

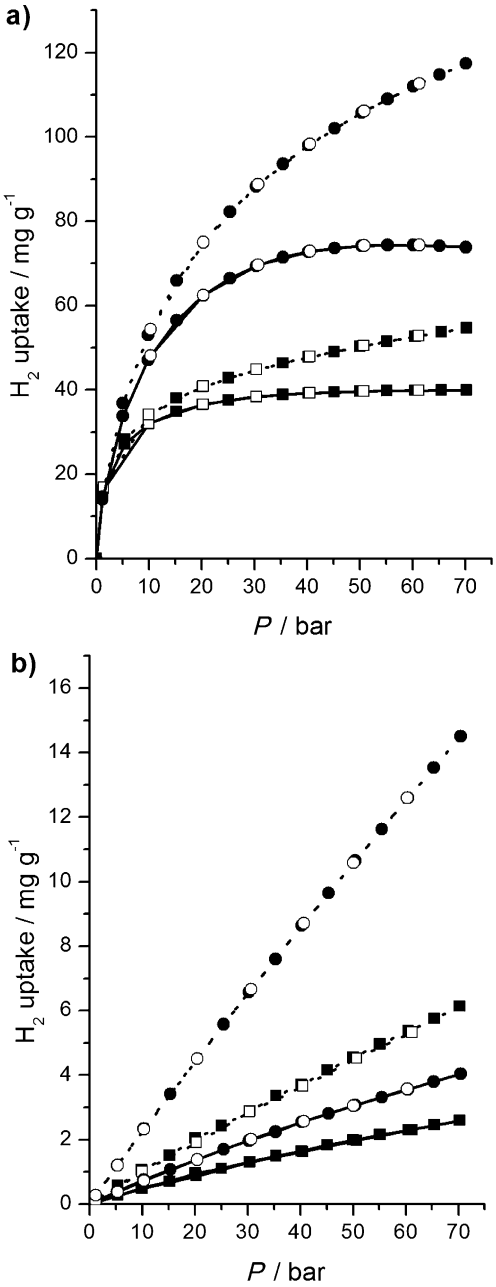

Figure 6. High-pressure gas-adsorption isotherms of **SNU-70′** (●, ○) and **SNU-71′** (■, □) for H_2 at a) 77, and b) 298 K. ——: excess uptake; -----: total uptake; filled shapes: adsorption; open shapes: desorption.

similar conditions.[17] However, at 298 K and 1 atm, the CO_2 uptake capacity of **SNU-71′** becomes 1.3 times greater than that of **SNU-70′** (35 mg g^{-1} in **SNU-70′** and 46 mg g^{-1} in **SNU-71′**). There have been some MOFs that adsorb CO_2 with high uptake capacity and high selectivity, such as SNU-M10 (9.2 wt %),[18] SNU-21S (11.1 wt %),[19] and Mg_2(dobdc) (35.2 wt %).[20] At 298 K and 45 bar, **SNU-70′** adsorbs CO_2 with an excess 1420 mg g^{-1} (total 1640 mg g^{-1}; Figure S3 in the Supporting Information), which is comparable to that of MOF-177 (excess 1493 mg g^{-1}, total 1656 mg g^{-1} at 298 K and 42 bar).[21] The reported highest excess CO_2 uptake capacities at 298 K and high pressures are 2400 mg g^{-1} at 50 bar for MOF-200 and MOF-210,[1] 2043 mg g^{-1} at 298 K and 40 bar for NU-100.[12] The isosteric heats of CO_2 adsorption in **SNU-70′** and **SNU-71′** are 17.2 and 17.8 kJ mol^{-1}, respectively, as calculated from the isotherms measured at 195, 273, and 298 K up to 1 atm by using the Clausius–Clapeyron equation.

The CH_4 adsorption isotherms show relatively high adsorption capacities. At 195 and at 298 K and up to 1 atm, **SNU-71′** shows slightly higher CH_4 uptake than **SNU-70′** (Figure 8), similar to the results for H_2 adsorption at 77 K and $P<1$ atm. The zero coverage isosteric heats of CH_4 adsorption in **SNU-70′** and **SNU-71′** are 9.4 and 14.6 kJ mol^{-1},

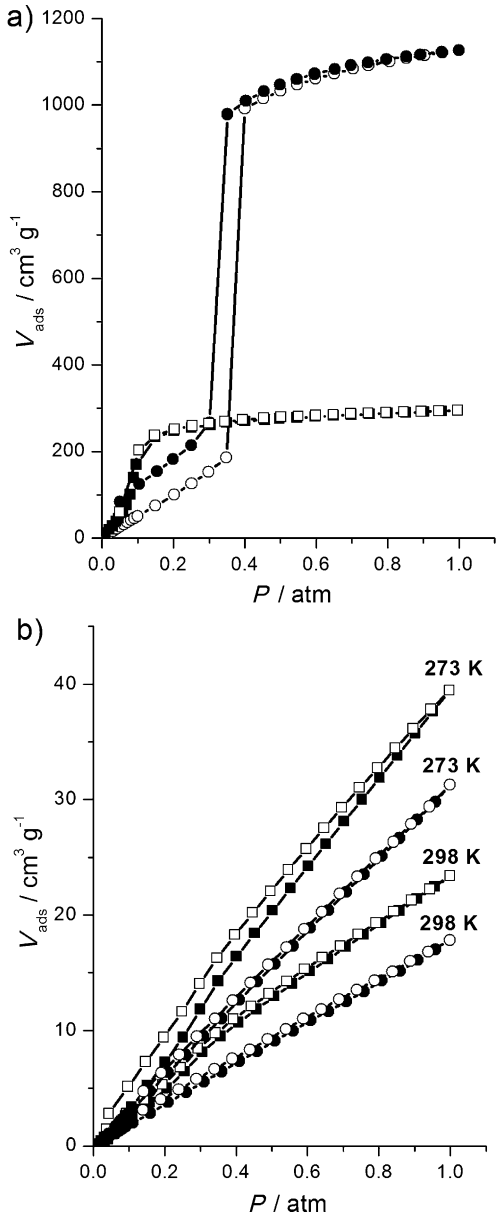

Figure 7. The gas-adsorption isotherms of **SNU-70′** (●, ○) and **SNU-71′** (■, □) for CO_2 at: a) 195, and b) 273 and 298 K. Filled shapes: adsorption; open shapes: desorption.

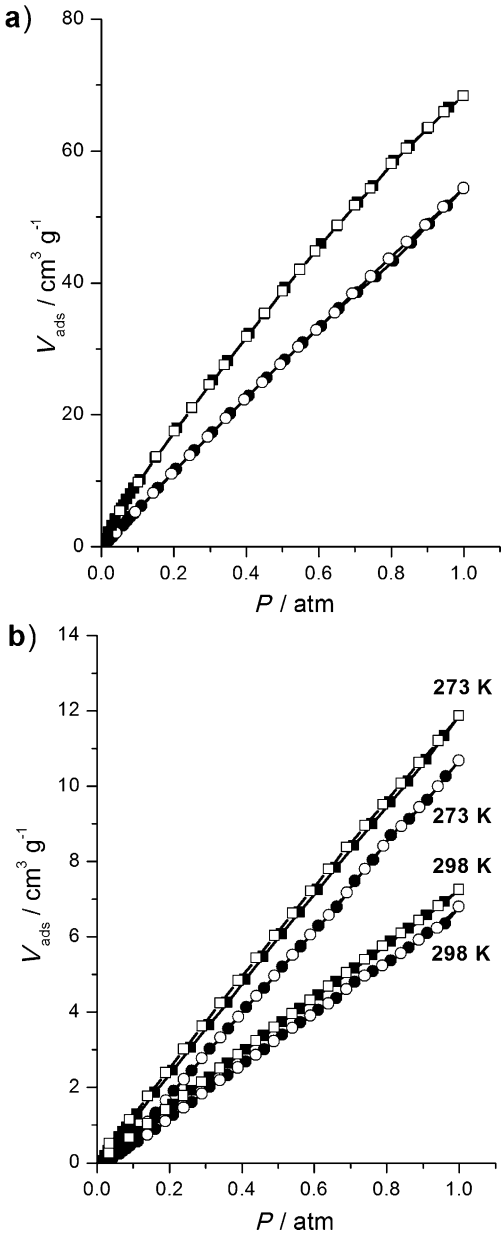

Figure 8. The gas-adsorption isotherms of **SNU-70′** (●, ○) and **SNU-71′** (■, □) for CH_4 at: a) 195, and b) 273 and 298 K. Filled shapes: adsorption; open shapes: desorption.

respectively. However, at 298 K and 45 bar, the CH_4 uptake capacity of **SNU-70′** (excess 168 mg g^{-1}, total 224 mg g^{-1}) are much higher than those of **SNU-71′** (excess 101 mg g^{-1}, total 121 mg g^{-1}; Figure S4 in the Supporting Information).

Post-synthetic bromination of SNU-70: The C=C double bond in the ligand of **SNU-70** was brominated at room temperature, then dried by using supercritical CO_2 to give **SNU-70 Br**. The elemental analysis data and the NMR spectra measured in [D_6]DMSO for the crystals that were digested in DCl indicated that all C=C bonds in **SNU-70** were brominated (see Figure S5 in the Supporting Information). Previously, it was reported that the C=C bonds in a MOF were partially brominated at room temperature in 24 h, and quantitative bromination was possible only at 100 °C.[22] In the present case, the diffusion of Br_2 into the pores must be much easier due to the very large pore size of **SNU-70**, which leads to more efficient bromination even at room temperature. For **SNU-70 Br**, the BET surface area is 2285 m^2 g^{-1} (Langmuir 2550 m^2 g^{-1}) and the pore volume is 0.908 cm^3 g^{-1}, which indicates that it still retains high porosity, although its porosity is reduced compared with that of **SNU-70′. SNU-70 Br** has H_2 uptake capacities of 7.3 mg g^{-1} at 77 K and 1 atm and 4.2 mg g^{-1} at 87 K and 1 atm (Figure 9). The isosteric heat of the H_2 adsorption is 6.14 to 4.41 kJ mol^{-1}, which is slightly higher than that of **SNU-70′**.

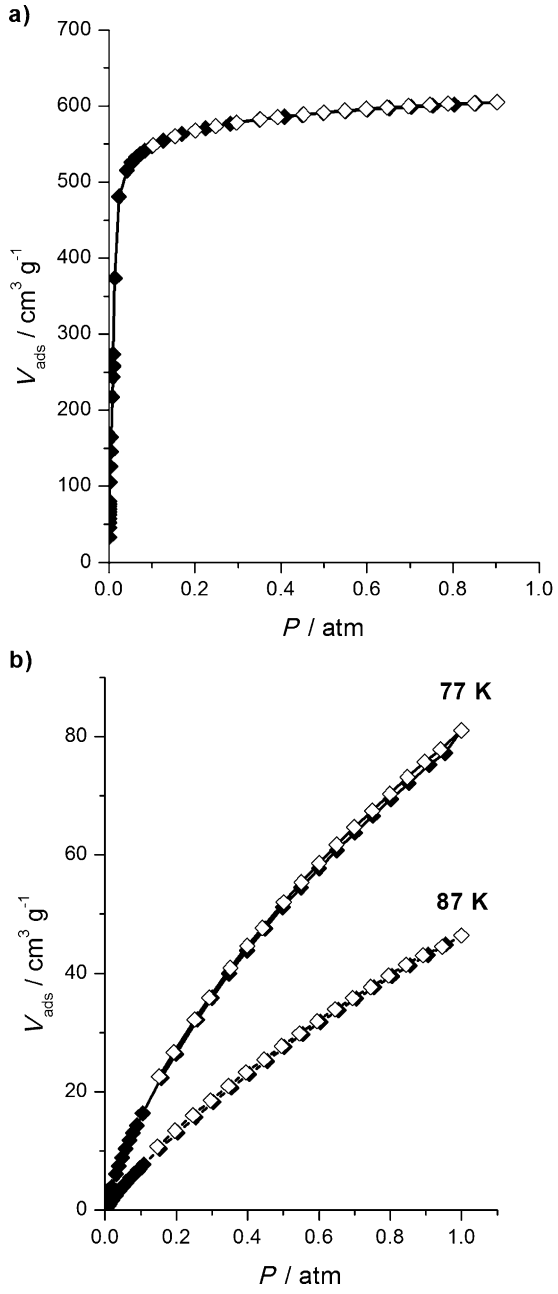

Figure 9. The adsorption isotherms of **SNU-70Br′** for: a) N_2 at 77 K, and b) H_2 at 77 and 87 K. Filled shapes: adsorption; open shapes: desorption.

Conclusion

The present study demonstrates that the interpenetration of MOFs with almost-identical network structures can be controlled by a simple change in the ligand, that is, the presence of a C=C or a C–C bond. Comparison of the gas-sorption properties indicate that the noninterpenetrated structure (**SNU-70′**) exhibits generally much higher gas adsorption capacities than the interpenetrated structure (**SNU-71′**) at high pressures regardless of the temperature, whereas the opposite is observed at low pressures due to the higher isosteric heats of the gas adsorption resulting from the smaller pores. In particular, the **SNU-70′** sample shows an extraordinarily high surface area and exceptionally high H_2 and CO_2 gas-sorption capacities. However, it should be noted here that gas-sorption properties cannot be easily predicted from the interpenetration. As seen in Figures 5 and 8, at $P<1$ atm, the gas-adsorption capacities for N_2 at 77 K and CO_2 at 195 K are higher for noninterpenetrated **SNU-70′** than interpenetrated **SNU-71′**, but H_2 and CH_4 adsorptions are the reverse, that is, **SNU-71′** has higher uptake capacities than **SNU-70′**. By a post-synthetic method, the C=C bonds in **SNU-70** were quantitatively brominated at room temperature and a noninterpenetrated MOF with a C–C bond in the ligand, which still shows a high porosity (BET 2285 $m^2 g^{-1}$; pore volume 0.908 $cm^3 g^{-1}$), was also successfully constructed. The present results might be useful for future construction of highly porous MOFs with interpenetration that may be controlled by a small change in the ligand to fine-tune the gas-sorption properties.

Experimental Section

Synthesis of ligands: 4-(2-Carboxyvinyl)benzoic acid (H_2CVB) and 4-(2-carboxyethyl)benzoic acid (H_2CEB) were synthesized by using previously reported procedures (see the Supporting Information).[23]

$[Zn_4O(CVB)_3]\cdot 13DEF\cdot 2H_2O$ (SNU-70): $[Zn(NO_3)_2]\cdot 6H_2O$ (0.030 g, 0.101 mmol) and H_2CVB (0.015 g, 0.075 mmol) were dissolved in DEF (5 mL) in a glass bottle, which was sealed and heated at 105 °C for 12 h in a programmable furnace. Pale-yellow cubic crystals were formed, which were filtered and washed with DEF (yield: 0.030 g, 55 %). FTIR (KBr pellet): $\tilde{\nu}=1667$ (DEF), 1607 cm^{-1} (carboxylate); elemental analysis calcd (%) for $C_{95}H_{165}N_{13}O_{28}Zn_4$: C 51.89, H 7.56. N 8.28; found: C 52.26, H 8.10, N 8.87.

$[Zn_4O(CEB)_3]\cdot 6DEF\cdot H_2O$ (SNU-71): $[Zn(NO_3)_2]\cdot 6H_2O$ (0.030 g, 0.101 mmol) and H_2CEB (0.015 g, 0.075 mmol) were dissolved in DEF (5 mL) in a glass bottle, which was sealed and heated at 105 °C for 12 h in a programmable furnace. Pale-yellow cubic crystals were formed, which were filtered and washed with DEF (yield: 0.020 g, 55 %). FTIR (KBr pellet): $\tilde{\nu}=1670$ (DEF), 1609 cm^{-1} (carboxylate); elemental analysis calcd (%) for $C_{60}H_{92}N_6O_{20}Zn_4$: C 48.72, H 6.27, N 5.68; found: C 49.83, H 6.05, N 5.63.

X-ray crystallography: X-ray data were collected by using an Enraf Nonius Kappa CCD diffractometer with graphite-monochromated $Mo_{K\alpha}$ radiation ($\lambda=0.71073$ Å) at 298 K. The respective crystals were sealed in a glass capillary together with the mother liquor. Preliminary orientation matrixes and unit cell parameters were obtained from the peaks of the first ten frames and then refined by using the whole data set. Frames were integrated and corrected for Lorentz and polarization effects by using DENZO.[29] The scaling and global refinement of crystal parameters were performed by SCALEPACK.[29] The structure was solved by using SHELXS-97[30] and full-matrix least-squares refinement against F^2 was carried out by using SHELXL-97.[30] All ring hydrogen atoms were assigned on the basis of geometrical considerations and allowed to ride upon the respective carbon atoms. The unsymmetrical dicarboxylate linkers are randomly oriented and the long and short parts cannot be differentiated from the benzene ring; the structures were refined by providing the appropriate occupancy factors. The solvent molecules could not be located from the difference maps, and the residual electron density corresponding to the solvent molecules was removed by using SQUEEZE[31] in the PLATON software.[32] The formulae of both **SNU-70** and **SNU-71** were determined from elemental analyses and TGA data.

Crystal data for SNU-70: $C_{95}H_{165}N_{13}O_{28}Zn_4$; pale-yellow cubic crystal ($0.2\times0.2\times0.2$ mm); $Fm\bar{3}m$; $a=30.234(4)$ Å; $V=27637(6)$ Å^3; $Z=8$; $T=$

298(2) K; $\rho_{calcd} = 0.411\ g\,cm^{-3}$; $\mu = 0.701\ cm^{-1}$; $F(000) = 3424$. A total of 214 reflections were collected, of which 214 were unique. Final $R_1(wR_2) = 0.0869(0.2640)$ with GOF = 1.203.

Crystal data for SNU-71: $C_{60}H_{92}N_6O_{20}Zn_4$; pale-yellow cubic crystals ($0.3 \times 0.3 \times 0.3$ mm); $I\bar{4}3m$; $a = 15.031(1)$ Å; $V = 3396.0(5)$ Å^3; $Z = 8$; $T = 298(2)$ K; $\rho_{calcd} = 0.835\ g\,cm^{-3}$; $\mu = 1.427\ cm^{-1}$; $F(000) = 856$. A total of 1020 reflections were collected, of which 606 were unique. Final $R_1(wR_2) = 0.0777(0.1820)$ with GOF = 0.830.

CCDC-846935 (**SNU-70**) and -846936 (**SNU-71**) contain the supplementary crystallographic data for this paper. These data can be obtained free of charge from The Cambridge Crystallographic Data Centre via www.ccdc.cam.ac.uk/data_request/cif.

Activation of MOFs with supercritical CO_2: Crystals of as-synthesized MOFs (≈0.3 g) were placed inside a supercritical dryer together with DEF and the drying chamber was sealed. The temperature and pressure of the chamber were increased to 40 °C and 200 bar with CO_2. The chamber was vented at a rate of 10 mL min^{-1} and then filled with CO_2 again. The cycles of refilling with CO_2, pressurizing, and venting were repeated for 24 h. After drying, the closed container was transferred to a glovebox filled with argon and transferred to a gas-sorption cell. The gas sorption isotherms were measured without further activation. Elemental analysis calcd (%) for $C_{30}H_{18}O_{13}Zn_4$ (**SNU-70′**): C 42.49, H 2.14; found: C 42.62, H 2.29; elemental analysis calcd (%) for $C_{30}H_{24}O_{13}Zn_4$ (**SNU-71′**): C 42.19, H 2.83; found: C 42.00, H 2.85.

Simulation of PXRD pattern of SNU-71′: The simulation of the rearrangement between the interpenetrated framework of **SNU-71** upon guest removal (**SNU-71′**) was modeled by using the Materials Studio program.[11] Indexing and refinement of the structure was not performed due to the low resolution of the PXRD pattern. Instead, various possible positions of the interpenetrated framework were modeled by moving the frameworks manually, and the PXRD pattern obtained from the Reflux module was compared with the experimental pattern.

Post-synthetic bromination of SNU-70: The guest molecules of **SNU-70** were exchanged for CH_2Cl_2. The guest-exchanged crystals (100 mg) were immersed in CH_2Cl_2 (10 mL), and liquid Br_2 (100 μL) was added at RT. After 1 d, unreacted Br_2 and CH_2Cl_2 were decanted off and the crystals were washed several times with fresh CH_2Cl_2, then stored in CH_2Cl_2. Elemental analysis data for the desolvated sample by using supercritical CO_2 indicate that all C=C double bonds of the ligand in **SNU-70** were brominated. ^{1}H NMR (300 MHz, DCl/[D$_6$]DMSO, 25 °C): $\delta = 7.72$ (d, $J = 7.9$ Hz, 2H; Ar-H), 7.44 (d, $J = 7.9$ Hz, 2H; Ar-H), 4.95 (d, $J = 11.9$ Hz, 1H; CBr-H), 5.20 ppm (d, $J = 11.7$ Hz, 1H; CBr-H); elemental analysis calcd (%) for $C_{30}H_{18}Br_6O_{13}Zn_4$ (**SNU-70Br**): C 27.14, H 1.37; found: C 26.94, H 1.27.

Gas sorption measurements: Low-pressure gas adsorption–desorption measurements were performed by using Autosorb-1 or Autosorb-3B (Quantachrome Instruments). All gases used in the studies were of 99.999 % purity. Before and after gas-sorption measurement, the sample weight was measured precisely. The surface area and total pore volume were determined from the N_2 gas isotherm at 77 K. The high-pressure sorption was measured for H_2 (77 K, 298 K), CO_2 (298 K), and CH_4 (298 K) in the range of 1–70 bar by the gravimetric method using a Rubotherm magnetic suspension balance. The trace water impurity was removed by passing the gases through a drying trap (model 500) filled with molecular sieve (5 Å), which was purchased from the Chromatography Research Supplies. The dried crystals (≈0.8 g) prepared by using supercritical CO_2 were transferred to the instrument and kept under vacuum for at least 3 h. All data were corrected for the buoyancy of the system and sample. The sample density used in the buoyancy correction was determined from the He displacement isotherms (up to 60 bar) measured at 298 K.

Acknowledgements

This work was supported by a National Research Foundation of Korea (NRF) Grant funded by the Korean Government (MEST; nos.: 2011-0031432 and 2012-0000651).

[1] H. Furukawa, N. Ko, Y. B. Go, N. Aratani, S. B. Choi, E. Choi, A. Ö. Yazaydin, R. Q. Snurr, M. O'Keeffe, J. Kim, O. M. Yaghi, *Science* **2010**, *329*, 424–428.

[2] a) M. P. Suh, H. J. Park, T. K. Prasad, D.-W. Lim, *Chem. Rev.* **2012**, *112*, 782–835; b) L. J. Murray, M. Dincă, J. R. Long, *Chem. Soc. Rev.* **2009**, *38*, 1294–1314; c) J.-R. Li, R. J. Kuppler, H.-C. Zhou, *Chem. Soc. Rev.* **2009**, *38*, 1477–1504; d) J. L. C. Rowsell, O. M. Yaghi, *J. Am. Chem. Soc.* **2006**, *128*, 1304–1315.

[3] a) Y.-G. Lee, H. R. Moon, Y. E. Cheon, M. P. Suh, *Angew. Chem.* **2008**, *120*, 7855–7859; *Angew. Chem. Int. Ed.* **2008**, *47*, 7741–7745; <lit b> Y. E. Cheon, M. P. Suh, *Angew. Chem.* **2009**, *121*, 2943–2947; *Angew. Chem. Int. Ed.* **2009**, *48*, 2899–2903; c) M. P. Suh, Y. E. Cheon, E. Y. Lee, *Coord. Chem. Rev.* **2008**, *252*, 1007–1026.

[4] a) S. Ma, J. Eckert, P. M. Forster, J. W. Yoon, Y. K. Hwang, J.-S. Chang, C. D. Collier, J. B. Parise, H.-C. Zhou, *J. Am. Chem. Soc.* **2008**, *130*, 15896–15902; b) S. Ma, D. Sun, M. Ambrgio, J. A. Fillinger, S. Parkin, H.-C. Zhou, *J. Am. Chem. Soc.* **2007**, *129*, 1858–1859.

[5] O. Shekhah, H. Wang, M. Paradinas, C. Ocal, B. Schupbach, A. Terfort, D. Zacher, R. A. Fischer, C. Woll, *Nat. Mater.* **2009**, *8*, 481–484.

[6] O. K. Farha, C. D. Malliakas, M. G. Kanatzidis, J. T. Hupp, *J. Am. Chem. Soc.* **2010**, *132*, 950–952.

[7] a) M. Dincă, A. Dailly, C. Tsay, J. R. Long, *Inorg. Chem.* **2008**, *47*, 11–13; b) M. Eddaoudi, J. Kim, N. Rosi, D. Vodak, J. Wachter, M. O'Keeffe, O. M. Yaghi, *Science* **2002**, *295*, 469–472.

[8] J. Zhang, L. Wojtas, R. W. Larsen, M. Eddaoudi, M. J. Zaworotko, *J. Am. Chem. Soc.* **2009**, *131*, 17040–17041.

[9] a) P. Ryan, L. J. Broadbelt, R. Q. Snurr, *Chem. Commun.* **2008**, 4132–4134; b) H. Frost, R. Q. Snurr, *J. Phys. Chem. C* **2007**, *111*, 18794–18803; c) D. H. Jung, D. Kim, T. B. Lee, S. B. Choi, H. Yoon, J. Kim, K. Choi, S.-H. Choi, *J. Phys. Chem. B* **2006**, *110*, 22987–22990.

[10] a) H. J. Choi, M. P. Suh, *J. Am. Chem. Soc.* **2004**, *126*, 15844–15851; b) E. Y. Lee, S. Y. Jang, M. P. Suh, *J. Am. Chem. Soc.* **2005**, *127*, 6374–6381; c) T. K. Maji, R. Matsuda, S. Kitagawa, *Nat. Mater.* **2007**, *6*, 142–148; d) S. Bureekaew, H. Sato, R. Matsuda, Y. Kubota, R. Hirose, J. Kim, K. Kato, M. Takata, S. Kitagawa, *Angew. Chem.* **2010**, *122*, 7826–7830; *Angew. Chem. Int. Ed.* **2010**, *49*, 7660–7664.

[11] *Materials Studio*, Version 5.0, Accelrys Inc., San Diego, CA (USA), **2009**.

[12] O. K. Farha, A. Ö. Yazaydin, I. Eryazici, C. D. Malliakas, B. G. Hauser, M. G. Kanatzidis, S. T. Nguyen, R. Q. Snurr, J. T. Hupp, *Nat. Chem.* **2010**, *2*, 944–948.

[13] a) M. Dincă, A. Dailly, Y. Liu, C. M. Brown, D. A. Neumann, J. R. Long, *J. Am. Chem. Soc.* **2006**, *128*, 16876–16883; b) L. Czepirski, J. Jagiello, *Chem. Eng. Sci.* **1989**, *44*, 797–801.

[14] a) H. Frost, T. Düren, R. Q. Snurr, *J. Phys. Chem. B* **2006**, *110*, 9565–9570; b) T. A. Makal, A. A. Yakovenko, H.-C. Zhou, *J. Phys. Chem. Lett.* **2011**, *2*, 1682–1689.

[15] H. J. Park, D.-W. Lim, W. S. Yang, T.-R. Oh, M. P. Suh, *Chem. Eur. J.* **2011**, *17*, 7251–7260.

[16] K. S. Walton, A. R. Millward, D. Dubbeldam, H. Frost, J. J. Low, O. M. Yaghi, R. Q. Snurr, *J. Am. Chem. Soc.* **2008**, *130*, 406–407.

[17] K. M. Choi, H. J. Jeon, J. K. Kang, O. M. Yaghi, *J. Am. Chem. Soc.* **2011**, *133*, 11920–11923.

[18] H.-S. Choi, M. P. Suh, *Angew. Chem.* **2009**, *121*, 6997–7001; *Angew. Chem. Int. Ed.* **2009**, *48*, 6865–6869.

[19] T. K. Kim, M. P. Suh, *Chem. Commun.* **2011**, *47*, 4258–4260.

[20] S. R. Caskey, A. G. Wong-Foy, A. J. Matzger, *J. Am. Chem. Soc.* **2008**, *130*, 10870–10871.

[21] A. R. Millward, O. M. Yaghi, *J. Am. Chem. Soc.* **2005**, *127*, 17998–17999.

[22] S. C. Jones, C. A. Bauer, *J. Am. Chem. Soc.* **2009**, *131*, 12516–12517.
[23] a) R. Kluger, L. Shen, H. Xiao, R. T. Jones, *J. Am. Chem. Soc.* **1996**, *118*, 8782–8786; b) P. Leighton, J. K. M. Sanders, *J. Chem. Soc. Perkin Trans. 1* **1987**, 2385–2393.
[24] D. Yuan, D. Zhao, D. Sun, H.-C. Zhou, *Angew. Chem.* **2010**, *122*, 5485–5489; *Angew. Chem. Int. Ed.* **2010**, *49*, 5357–5361.
[25] J.-S. Choi, W.-J. Son, J. Kim, W.-S. Ahn, *Microporous Mesoporous Mater.* **2008**, *116*, 727–731.
[26] W. Zhou, H. Wu, M. R. Hartman, T. Yildirim, *J. Phys. Chem. C* **2007**, *111*, 16131–16137.
[27] J. L. Rowsell, A. R. Millward, K. S. Park, O. M. Yaghi, *J. Am. Chem. Soc.* **2004**, *126*, 5666–5667.
[28] J. A. Mason, K. Sumida, Z. R. Herm, R. Krishna, J. R. Long, *Energy Environ. Sci.* **2011**, *4*, 3030–3040.
[29] Z. Otwinowski, W. Minor, in *Processing of X-ray Diffraction Data Collected in Oscillation Mode, Methods in Enzymology, Vol. 276, Macromolecular Crystallography, Part A* (Eds.: C. W. Carter, Jr., R. M. Sweet), Academic Press, **1997**, pp. 307–326.
[30] G. M. Sheldrick, SHELX-97: Programs for Crystal Structure Analysis, University of Göttingen, Göttingen, Germany, **1997**.
[31] P. van der Sluis, A. L. Spek, *Acta Crystallogr. A* **1990**, *46*, 194–201.
[32] a) A. L. Spek, *Acta Crystallogr. A* **1990**, *46*, C34; b) A. L. Spek, PLATON, A Multipurpose Crystallographic Tool, Utrecht University, Utrecht, The Netherlands, **1998**.

Received: February 12, 2012
Published online: June 8, 2012

